Cerebral Cortex September 2014;24:2401–2408
doi:10.1093/cercor/bht092
Advance Access publication April 16, 2013

Where Is Human V4? Predicting the Location of hV4 and VO1 from Cortical Folding

Nathan Witthoft[1], Mai Lin Nguyen[1,3], Golijeh Golarai[1], Karen F. LaRocque[1], Alina Liberman[1,4], Mary E. Smith[1,5] and Kalanit Grill-Spector[1,2]

[1]Department of Psychology and [2]Neuroscience Institute, Stanford University, Stanford, CA, USA, [3]Department of Psychology, University of Cambridge, Cambridge, UK, [4]Helen Wills Neuroscience Institute, University of California at Berkeley, Berkeley, CA 94720, USA and [5]Department of Psychology, University of California at San Diego, La Jolla, CA 92093, USA

Address correspondence to Dr Nathan Witthoft. Email: witthoft@stanford.edu

A strong relationship between cortical folding and the location of primary sensory areas in the human brain is well established. However, it is unknown if coupling between functional responses and gross anatomy is found at higher stages of sensory processing. We examined the relationship between cortical folding and the location of the retinotopic maps hV4 and VO1, which are intermediate stages in the human ventral visual processing stream. Our data show a consistent arrangement of the eccentricity maps within hV4 and VO1 with respect to anatomy, with the consequence that the hV4/VO1 boundary is found consistently in the posterior transverse collateral sulcus (ptCoS) despite individual variability in map size and cortical folding. Understanding this relationship allowed us to predict the location of visual areas hV4 and VO1 in a separate set of individuals, using only their anatomies, with >85% accuracy. These findings have important implications for understanding the relation between cortical folding and functional maps as well as for defining visual areas from anatomical landmarks alone.

Keywords: cortical folding, functional neuroanatomy, retinotopy, ventral visual stream, visual cortex

Introduction

Prior research documents a strong relationship between cortical folding and the location of primary sensory areas in the human brain (Rademacher et al. 1993) as well as visual areas that are myelinated early in development such as hMT (Dumoulin et al. 2000). For example, the first cortical visual area, V1, is always found in the calcarine sulcus (Dougherty et al. 2003; Benson et al. 2012). However, it is uncertain how specific a relationship between gross anatomy and functional maps obtains in parts of visual cortex further along in the hierarchy of visual processing (Hasnain et al. 2001).

hV4 and VO1 are adjacent retinotopic maps, each representing the contralateral visual hemifield (Brewer et al. 2005), found in a sizeable anatomical expanse bounded by the posterior fusiform gyrus and extending medially to the collateral sulcus and posteriorly to the lingual gyrus. While injuries that compromise this part of the brain can often result in visual field cuts consistent with the underlying retinotopy, damage here can also produce more complex perceptual deficits such as achromatopsia, prosopagnosia, or some combination of these (Meadows 1974; Bouvier and Engel 2006). Given that functional magnetic resonance imaging (fMRI) experiments have also shown that the anterior parts of this anatomical region are highly responsive to color (McKeefry and Zeki 1997) and faces (Kanwisher et al. 1997), the prevailing view is that neurons in this part of the brain serve an important role in intermediate processing in the visual ventral stream hierarchy.

By examining the location of retinotopic maps on 11 individual subjects' anatomies, we found that hV4 and VO1 have a regular relationship to the cortical folding of the ventral surface of the brain, and that their boundary lies in the posterior transverse collateral sulcus (ptCoS) at the location where 2 separate eccentricity maps meet. This relationship between function and anatomy is present in over 90% of hemispheres, enabling us to accurately predict the location of the hV4/VO1 boundary in a second set of 10 new subjects from their anatomy alone, despite variation in the size of the maps and the exact pattern of cortical folding across subjects.

Materials and Methods

Subjects

Retinotopy data from 11 subjects (4 males), ages 18–36 years was used for the first dataset and data from an additional 10 subjects (8 males) ages 22–57 years comprised the second test set. These MR scans used a 3T GE scanner located at the Lucas Center for Imaging (20 subjects) or the Center for Cognitive and Neurobiological Imaging (1 subject) at Stanford University. All subjects had normal or corrected-to-normal vision and provided written, informed consent. Protocols were approved by the Stanford Internal Review Board on Human Subjects Research.

Data Acquisition

Anatomical Scans

Two to 4 high-resolution, whole-brain anatomy scans were obtained for each subject using an 8-channel whole-brain coil and T_1-weighted SPGR scans (TR = 1000 ms, flip angle = 45°, FOV = 200 mm, voxel size: 0.938 × 0.938 × 1.5 mm, 166 sagittal slices). These runs were then averaged to form a high-quality whole-brain volume for each subject.

Functional Scans

Functional scans were obtained using an 8-channel phased-array surface coil (Nova Medical, Inc., Wilmington, MA, USA). In all experiments, 32 oblique slices extending from the occipital pole to the anterior temporal lobe were obtained. These slices were oriented perpendicular to the calcarine sulcus. Data were collected using a T_{2}*-weighted gradient echo spiral pulse sequence (Glover and Law 2001) with the following parameters: TR = 2000 ms or TR = 1500 ms, TE = 30 ms, flip angle = 76°, FOV = 200 mm, voxel size: ranged from 2.5 mm isotropic to 3.125 × 3.125 × 3 mm. The same prescription was used to obtain anatomical T_1-weighted images, which were later used to align functional data with the high-resolution anatomical volume of each subject. During MRI scanning, subjects lay supine in the bore of the magnet. Visual stimuli were projected onto a screen and viewed through an angled mirror mounted above the subject's head.

Traveling Wave Retinotopy

Eleven subjects (10 in set 1, 1 in set 2) participated in a standard traveling wave retinotopy paradigm (Engel et al. 1994; Brewer et al. 2005; Sayres and Grill-Spector 2008). Subjects were instructed to

fixate and press a button when the fixation color changed. Subjects participated in 2 runs where we measured polar angle preferences using a 45° wedge rotating clockwise about fixation 22.5° every 2 s and 2 runs where we measured eccentricity responses employing a series of traveling concentric rings (1.4° in diameter) centered at fixation. The innermost ring consisted of a disk with a diameter of ~2.8° while the most peripheral extent of the checkerboard stimuli was ~14–15° from fixation. Both the wedge and ring stimuli contained 100% contrast black and white phase reversing checkerboards (at a rate of 4 Hz) and used 6 cycles (either a full rotation of the wedge or a full expansion of the ring) each lasting 32 s. Each run contained 6 cycles, which were interspersed with 4 16-s blank periods (96 TRs in total). In addition, each scan began and ended with a blank 12-second block.

PRF Bar Retinotopy

Ten subjects (1 in set 1, 9 in set 2) participated in a pRF retinotopy paradigm (Dumoulin and Wandell 2008). Subjects took part in 4–10 runs in which they viewed a bar filled with 100% contrast phase reversing black and white checkerboards. Runs were either 128 1500 ms TRs (5 subjects), or 96 2000ms TRs (5 subjects). Subjects were instructed to fixate on the central point and perform a color discrimination task on the fixation cross. The bar moved smoothly across visual space in 8 different directions (4 cardinal directions plus 4 diagonals), completing each sweep in 24 s. Four times during each run, the bar disappeared, leaving a mean-luminance screen for 12 s. In addition, each scan began and ended with a blank 12-s block.

Data Analysis: Anatomy

Anatomy

The T_1 anatomical images of each subject were averaged together and segmented to white and gray matter using ITK-SNAP (http://white.stanford.edu/itkgray) in conjunction with the FreeSurfer autosegmentation (http://surfer.nmr.mgh.harvard.edu). A cortical surface mesh of each of our 42 hemispheres was created on the boundary of the white and gray matter and then partially "inflated" to aid visualization.

Identification of the Posterior Transverse Collateral Sulcus

The collateral sulcus is the long sulcus running along the ventromedial surface of the temporal lobe. At its posterior extent, the collateral sulcus often has a branch that runs laterally across the ventral surface forming the posterior boundary of the fusiform gyrus. This branch is the "posterior transverse collateral sulcus" (ptCoS).

The main features for locating the ptCoS are as follows:

1. Transverse to the posterior end of the collateral sulcus on the ventral surface
2. Forms the posterior boundary of the fusiform gyrus
3. Forms the anterior boundary of the inferior occipital gyrus
4. When viewing the ventromedial-inflated surface, the sulci generally appear in the following order: calcarine, lingual, and ptCoS, as one goes ventrally from the calcarine sulcus.

The Supplementary Materials provide a detailed guide to our method for labeling subjects' anatomies and are accompanied by additional example anatomies in Supplementary Figure S1. This guide is especially useful when the anatomical features of a particular brain are not obvious due to individual variability. For example, in some brains the ptCoS does not branch directly from the CoS, while in others, there may be more than one sulcus that appears to branch transversely from the CoS.

Data Analysis: fMRI

Except where otherwise mentioned, all data processing and analysis was done using mrVista (http://white.stanford.edu/mrvista) and MATLAB (mathworks.com).

fMRI: Preprocessing

Each subject's fMRI data were aligned to their high-resolution anatomical scans using inplane anatomical images taken with the same prescription. Functional images for each subject were motion corrected to remove small head motions during scans. The estimated motion for each of our subjects was <1.5 voxels (max = 1.2 voxels, min = 0.1 voxels), so no subjects were excluded on the basis of excessive motion. Time series data were filtered using a temporal high-pass filter with a 1/20 Hz cutoff and then converted to percentage signal change by dividing the time series of each voxel by its mean intensity.

Traveling Wave Retinotopy

A Fourier transform was applied to the time series from each voxel, and the phase offset of power at the stimulus frequency determined. The phase offset refers back to the stimulus, thus denoting the angle or eccentricity preference that produced an increased response in a voxel. The goodness of fit of the data to a sine wave can be assessed using a measure of coherence, which reflects the power at the stimulus frequency relative to the total power in the time series. Each voxel phase is determined separately for the eccentricity and polar angle scans, generating 2 mappings of the visual field along orthogonal axes.

PRF Retinotopy

We used a population receptive field (pRF) model (Dumoulin and Wandell 2008), to determine which pRF best describes each voxel's response to traveling bar stimuli. Each pRF is represented as a 2D Gaussian function in visual space, described by its center relative to the fovea and its standard deviation, reflecting its estimated size. The pRF analysis uses an optimization algorithm to estimate the pRF parameters that best fit the observed response for each voxel. This prediction is computed by multiplying the pRF with a binary mask of the stimulus position at each time point, and convolving the resulting series of amplitudes over time with a hemodynamic impulse response function. The solution is obtained in a 2-stage, coarse-to-fine optimization approach as described in (Dumoulin and Wandell 2008).

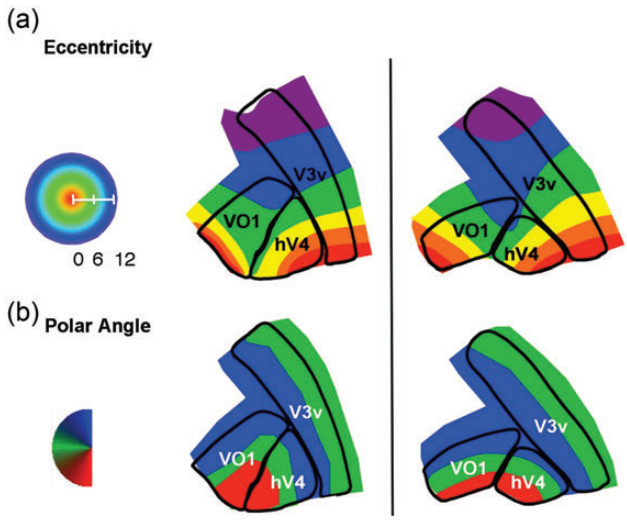

Figure 1. hV4 and VO1 share a polar angle representation but are on different eccentricity representations. Unlike the boundaries between areas V1 and hV4, the boundary between hV4 and VO1 is located at the reversal in eccentricity preference rather than polar angle preference. The shared polar angle representation may be bent such that the eccentricity boundary and the polar angle boundary roughly coincide (left column) or the polar angle representation may be fairly straight (right column). It is worth noting that hV4 does not extend along the entire upper vertical meridian represented in V3v.

Smoothing

Retinotopy data were smoothed for visualization on the meshes and for the figures used in the article. The smoothing procedure consisted of replacing each value on the mesh with the average of itself and its neighbors. This procedure was iterated twice.

Defining the hV4/VO1 Maps

hV4 and VO1 were defined following Brewer et al. (2005). That is, the retinotopic extent of hV4 in our data was generally found to cover a full hemifield. Unlike the maps surrounding the confluent fovea (V1–hV4), which share an eccentricity representation, and whose borders are defined by reversals in polar angle preference (Sereno et al. 1995), hV4 and VO1 share a polar angle representation, and their boundary is defined by a reversal in the eccentricity preference as illustrated in Figure 1 (see also Brewer et al. 2005; Hansen et al., 2007). In some cases, the lower vertical meridian of hV4 may be hard to image due to an MR artifact arising from the transverse sinus (referred to as the "venous eclipse" by Winawer et al. 2010). However, the sinus artifact tends to affect BOLD signals on the inferior occipital gyrus (IOG), and in our data, does not interfere with the BOLD signals in the ptCoS. We also note (Fig. 1) that the border hV4 shares with V3v does not extend as far into the periphery as V3v. In our observations, the peripheral parts of V3v representing the upper vertical meridian are adjacent to the peripheral parts of VO1 (Arcaro et al. 2009).

Cross Validation

For dataset 1, NW marked the ptCoS and defined the visual field maps. KGS validated the ptCoS marking and visual field map definitions. For test set 2, NW marked the ptCoS and KGS determined the hV4/VO1 boundary from the eccentricity map; NW then cross-validated retinotopic maps using polar angle and eccentricity maps.

Measurements of Distance Between the hV4/VO1 Boundary and the PtCoS

For each point along a given hV4/VO1 boundary, we measured its distance along the cortical surface to the nearest point in the fundus of the ptCoS. As the distribution of distances was non-normal, we used the median distance for each subject in each hemisphere as our measure of the distance between the ROIs. As the collection of median distances from across subjects was also non-normally distributed, we used the median of those as our summary measure. A 95% confidence interval around this median was generated using a bootstrapping procedure implemented with the MATLAB functions bootstat (which implements bootstrap with replacement) and bootci (which computes the confidence interval).

Results

The Large-Scale Eccentricity Map of the Ventral Visual Stream Is Aligned with Anatomy in a Systematic Way

We defined visual field maps in the ventral visual cortex of 11 subjects from dataset 1 (see Materials and Methods section). Retinotopy data were projected to the cortical surface reconstruction of each subject's anatomy, enabling us to consistently identify anatomical landmarks and examine the relation between these maps and cortical folding.

Figure 2*a* shows the relevant anatomy. Of particular interest is the ptCoS. It generally branches off at nearly a right angle from the posterior extent of the collateral sulcus, running medial to lateral (Duvernoy et al. 1991; Fig. 2*a*, and see Supplementary Material). While not described prominently in the fMRI literature, the fact that this sulcus divides the fusiform gyrus in the temporal lobe from the inferior occipital and lingual gyri in the occipital lobe makes it an important anatomical landmark (Huntgeburth and Petrides 2012). In our data, this sulcus was readily identified on the cortical surface of 20 of 22 hemispheres.

Figure 2*b* shows an anatomically restricted and unthresholded eccentricity map projected onto the cortical surface which helps visualize the relationship between the eccentricity map and cortical folding. The eccentricity map is entirely consistent with the organization described by Brewer and Wandell (Brewer et al. 2005) showing 2 large foveal representations (red-orange regions in Figs 2*b* and 3*a*, see Supplementary Figs S2 and S5). The posterior foveal representation, in the vicinity of the occipital pole, is referred to as the confluent fovea. The more anterior foveal representation, called the ventral–occipital (VO) fovea, generally lies on the medial bank of the posterior fusiform gyrus. This eccentricity structure, in which the representation of the periphery (here ~10–14°) extends medially from the VO fovea into the collateral sulcus (Arcaro et al. 2009) is widely agreed upon, despite disagreements on the representation of polar angle in hV4 (Hadjikhani et al. 1998; Tyler et al. 2005; Brewer et al. 2005; Hansen et al. 2007). As our stimulus only extended out to 14°, we cannot tell whether or not hV4 responds to more peripheral stimuli.

By examining the relationship between the eccentricity map and cortical folding in individual subjects, we found that the large-scale eccentricity map is aligned with the anatomy in a systematic way. First, there are 2 eccentricity representations, one emerging from the confluent fovea and the second emerging from the VO fovea. Second, these 2 eccentricity representations 'collide' in the ptCoS at mid to far eccentricities (Fig. 2*b*). This collision produces a reversal of the eccentricity map on the ptCoS. Focusing on the relationship between anatomical structure and function we might prefer to say that the ptCoS not only divides the occipital and temporal lobes, but also divides the confluent fovea and its associated visual field representations from the maps associated with the VO fovea.

The Boundary Between hV4 and VO1 is Located Within the Posterior Transverse Collateral Sulcus

Next we delineated retinotopic visual areas (Fig. 2*c*,*d*), marking the boundaries of ventral retinotopic maps hV4 and VO1 as described in Brewer et al. (2005). Unlike the maps surrounding the confluent fovea (V1–hV4), which share an eccentricity representation, and whose borders are defined by reversals in polar angle preference (Sereno et al. 1995), hV4 and VO1 share a polar angle representation, and their boundary is defined by a reversal in the eccentricity preference (Brewer et al. 2005; Hansen et al. 2007; Fig. 1). While there is variability in the bending of their polar angle map the reversal of the eccentricity map is a stable feature across subjects (compare left and right columns of Fig. 1). Our data show that this reversal in eccentricity preference almost always occurs in the ptCoS. That is, the boundary between the 2 maps lies in the ptCoS, with hV4 extending posteriorly onto the IOG toward the confluent fovea, and VO1 extending anteriorly onto the medial part of the posterior fusiform gyrus toward the VO fovea (Fig. 2*c*,*d*).

To quantify the functional–anatomical correspondence, we defined hV4 and VO1 in each subject using the retinotopic model shown in Figure 1, and then compared the boundary

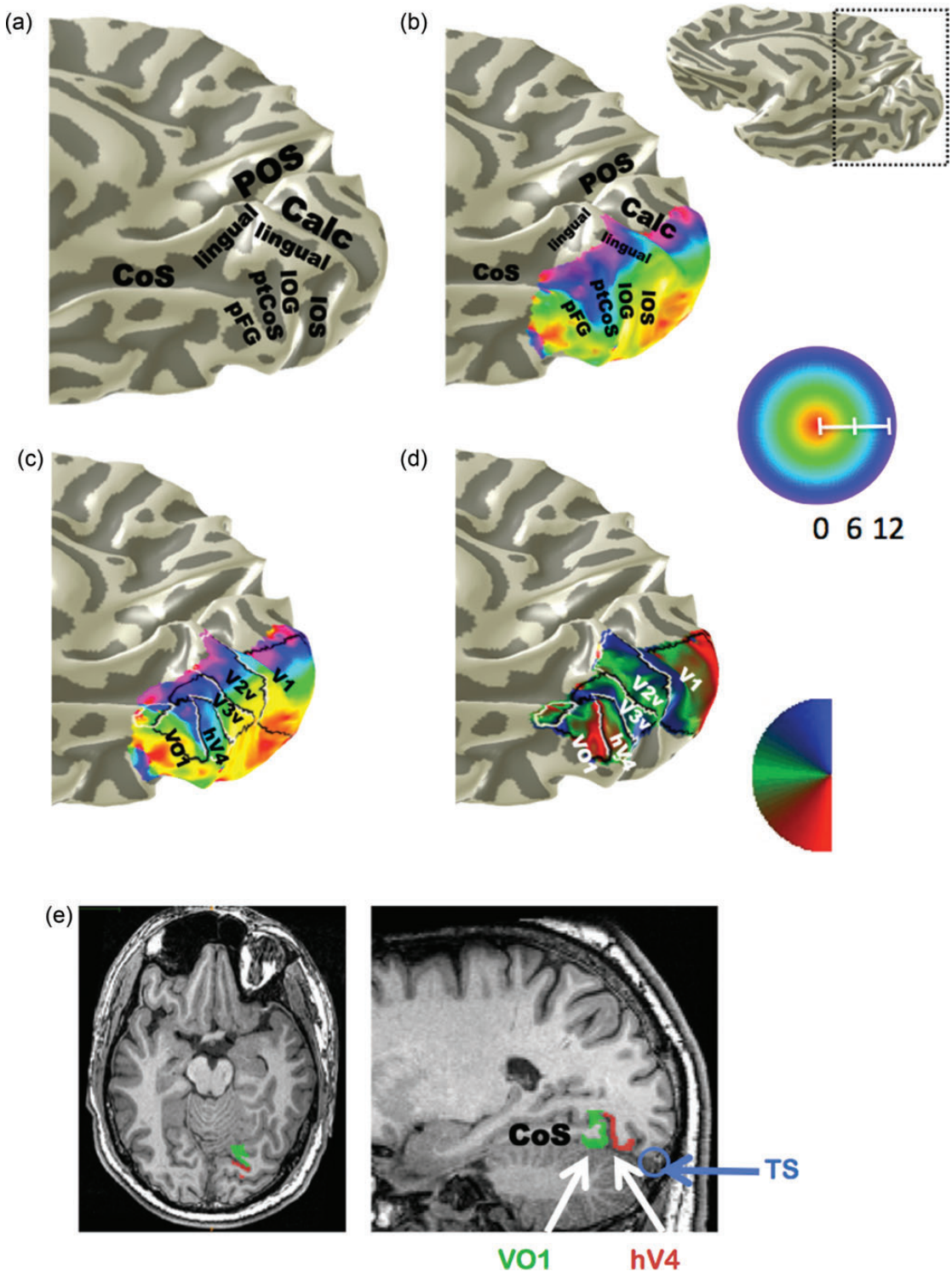

Figure 2. The posterior transverse collateral sulcus divides the confluent and VO eccentricity maps and is the location of the boundary between hV4 and VO1. (*a*) A ventromedial view of the posterior portion of the right hemisphere with anatomical labels. POS: parietal occipital sulcus; Calc: calcarine sulcus; Ling: lingual sulcus and gyrus; IOS: inferior occipital sulcus; IOG: inferior occipital gyrus; ptCoS: posterior transverse collateral sulcus; pFG: posterior fusiform gyrus; CoS: collateral sulcus. (*b*) The same hemisphere, but with an unthresholded eccentricity map restricted anatomically to the ventromedial surface of the posterior temporal and occipital lobes. There are 2 clear foveas, the posterior confluent fovea and a more anterior one (VO) located on the fusiform gyrus. Note how the eccentricity bands expanding outward from the 2 foveas "collide" in the ptCoS. (*c*) Same hemisphere with eccentricity map and boundaries of visual field maps. (*d*) Polar angle map on same hemisphere with visual field map boundaries. (*e*) Axial and sagittal views of the brain volume of the same hemisphere. In the axial view, the transverse nature of the sulcus is clearly visible, as is the fact that the visual field maps (hV4: red, VO1: green) lie on opposite sides of the sulcus. The sagittal view shows the collateral sulcus as well as the ptCoS and highlights both the depth of the ptCoS, and the way in which the hV4 and VO1 are wrapped around the neighboring gyri. The blue circle indicates the transverse sinus (TS), showing that it lies fairly distant from the ptCoS.

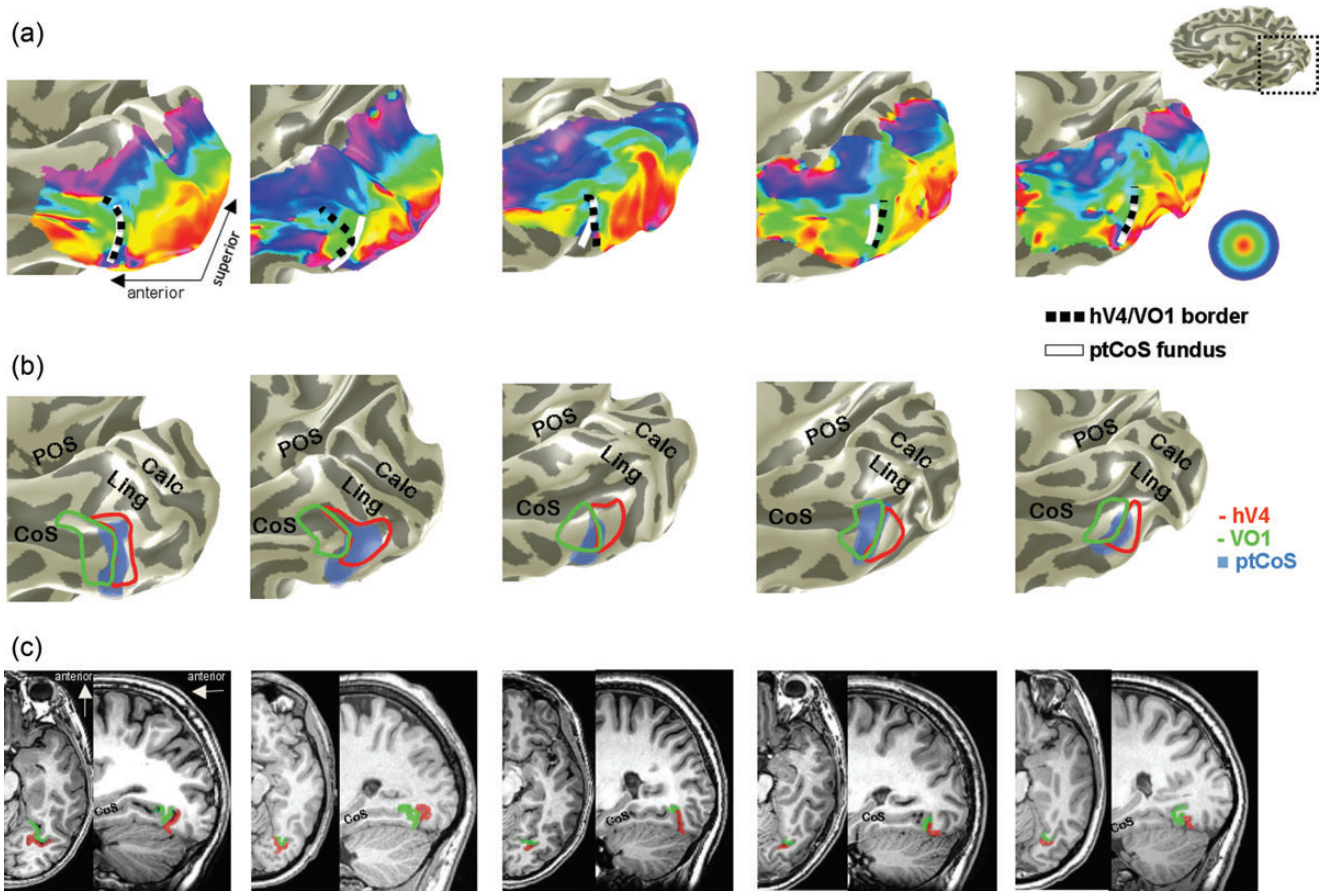

Figure 3. Examples showing boundary of hV4 and VO1 lies within the ptCoS. (*a*) Five right hemispheres showing the unthresholded eccentricity map restricted anatomically to the occipital lobe. In each case, the white line marking the fundus of the ptCoS lies between the confluent and VO foveas. The black dashed line is the boundary of hV4 and VO1. (*b*) Boundaries of hV4 and VO1 on the labeled anatomies of the same hemispheres with the ptCoS marked in blue gray. (*c*) Sagittal and axial views of the same hemispheres showing location of hV4 (red) and VO1 (green). In each axial, we illustrate the layout of the ptCoS such that it runs medial to lateral across the ventral surface and that hV4 and VO1 tend to be on opposite sides of the sulcus. The sagittal views show the collateral sulcus and posterior hippocampus for reference and, in some cases, make visible the way in which each of these regions is wrapped around a gyrus.

between these 2 maps to the location of the ptCoS. Notably, in all 20 of 22 hemispheres in which the ptCoS was easily identified, the boundary between hV4 and VO1 was located within the ptCoS, generally running along or near the fundus, with hV4 extending toward the confluent fovea on the IOG, and VO1 extending toward the VO fovea on the posterior fusiform gyrus (pFG, see Figs 2 and 3 for 6 example hemispheres, and see Supplementary Fig. S3 for all 22 hemispheres). In 1 of the 2 remaining hemispheres, the boundary between hV4 and VO1 was in a sulcus that could plausibly be the ptCoS (see Supplementary Fig. S3, subject 2, left hemisphere), while in the remaining hemisphere, the boundary was on a gyrus (see Supplementary Fig. S3, subject 5, left hemisphere).

As a second analysis, we measured the median distance along the cortical surface between the hV4/VO1 boundary and the ptCoS in each subject and hemisphere (see Materials and Methods). We then compared the data from the 2 hemispheres and found no significant difference in the median distance between the ptCoS and the border (median distance on left: 2.4 mm; median distance on right, 1.7 mm; Mann–Whitney *U*-test, $z = 1.1$ $P > 0.25$). Collapsing across subjects and hemispheres, we found that the median distance between the boundary and the ptCoS was 2.4 mm with a 95% confidence interval of 1.7–3.6 mm (see Materials and Methods section). Taken together, these analyses show a consistent relationship between intermediate-level visual field maps and cortical folding.

The Relationship Between Eccentricity Maps and Cortical Folding Changes Between Early and Intermediate Ventral Areas

It is interesting that the visual field maps hV4 and VO1 have a different spatial organization relative to cortical folding compared with the V1–V3 visual field maps. Figures 2*b* and 3*a* show that iso-eccentricity bands in V1 are arranged orthogonal to the calcarine sulcus. That is, the preferred eccentricity changes as one moves down the fundus of the calcarine sulcus, while the polar angle remains relatively constant. However, in hV4 and VO1, iso-eccentricity bands are arranged roughly parallel to the ptCoS. Moreover, because both hV4 and VO1 are wrapped around gyri (the IOG and medial aspect of the fusiform, respectively, see Figs 2*e* and 3*c*), the foveal and peripheral parts within each map are brought into close proximity. This wrapping of the hV4 and VO1 maps around gyri can be seen in every hemisphere (see Supplementary Fig. S4).

The Location of the Boundary Between hV4 and VO1 can be Predicted From the Anatomy Alone

Given the robust coupling between functional maps and anatomy in our first dataset, we asked whether it is possible to predict the location of the hV4/VO1 boundary from the anatomy alone. Here, we used independent anatomical and retinotopic data from 10 additional subjects (see Materials and Methods section). Using only the anatomical data, NW marked the fundus of the ptCoS (Fig. 4*a*, white line) in the 10 new subjects, without viewing the retinotopic maps. Independently, KGS marked the eccentricity reversal between the confluent and VO1 foveas (Fig. 4*b*, black line). We then tested whether the fundus of the ptCoS corresponded to the eccentricity reversal and consequently to the hV4 and VO1 boundary. The eccentricity reversal was found in the marked sulcus in 17 of 20 (85%) of the hemispheres (see Supplementary Fig. S5 for all hemispheres). Of the remaining 3 hemispheres, the ptCoS was likely misidentified in 2 subjects with atypical anatomy (see Supplementary Fig. S5, subject 1, left hemisphere and subject 4, right hemisphere), and on the remaining hemisphere the hV4/VO1 boundary was on a gyrus (see Supplementary Fig. S6, subject 8, left hemisphere). We then validated this analysis by defining hV4 and VO1 from both polar angle and eccentricity maps (Fig. 4*c* and see Supplementary Fig. S6), confirming that the boundary between these regions indeed runs along the ptCoS. This shows that in most cases, the boundary between hV4 and VO1 can reliably be located on the basis of anatomy alone, and that even when the anatomy is difficult to label, the boundary between hV4 and VO1 is generally in a sulcus that could plausibly be the ptCoS.

Discussion

Our data show that the ptCoS divides the occipital and temporal eccentricity representations in posterior visual cortex. Consequently, the boundary between hV4 and VO1 lies within the ptCoS closely overlapping its fundus in >90% of hemispheres. Using cortical surface visualizations and improved measurements on the cortical surface, our findings extend and clarify previous measurements of the relationship between anatomy and the location of intermediate visual areas, which were difficult to establish using volumetric analyses of functional–anatomical correspondence (Hasnain et al. 2001).

The ptCoS is a Useful Landmark for Defining Functional Regions in the Ventral Visual Cortex

How can we use this information in understanding the functional organization of ventral occipito-temporal cortex? The regular relationship between the retinotopy and the anatomy provides an additional robust constraint for the many researchers interested in defining visual field maps in the human brain. Further, our findings can contribute to the ongoing development of automated atlases (Benson et al. 2012) for defining these visual areas. Moreover, there is increasing evidence that functional regions defined by selective responses to specific categories such as faces and places relative to other visual stimuli, also have a regular relationship to both anatomy and visual field maps (Arcaro et al. 2009). For example, one can consistently find a face-selective activation on the IOG lateral to hV4 (Weiner and Grill-Spector 2010), such that the ptCoS separates it from face activations on the posterior fusiform gyrus. The mutual constraints observed between retinotopy, anatomy, and category selectivity can therefore be used to inform consistent decisions about how to identify and label functional regions and may provide insights into the nature of their computations. The importance of consistent labeling across subjects cannot be overstated, as the comparison of results across typical subjects, or across different groups of subjects, or across laboratories is entirely dependent on choosing regions of interest in the same manner across subjects and/or time.

The fact that hV4 and VO1 are consistently associated with the ptCoS could also prove useful in interpreting patient data, particularly when retinotopic maps and functional measurements are not available. As noted, many studies have shown that lesions within and in the vicinity of hV4 and VO1 are associated with visual field cuts, achromatopsia, prosopagnosia, and often some combination of these (Meadows 1974). One common approach to combining data from neuropsychological case studies is to normalize anatomical images to a template brain and then compute the region of lesion overlap across brains. While such an approach has been very revealing (Bouvier and Engel 2006), the fact that functional maps have a specific relation to the anatomy in this region of the brain may allow for comparison across subjects without normalization or averaging, or for deeper analysis of individual subject data.

The Strong Relationship Between the ptCoS and hV4/VO1 has Implications for Theories of Cortical Folding

Why should such a consistent relationship be observed between functional maps and cortical folding? While the pattern of sulci and gyri may be specified innately, it may also be that in visual cortex, cortical folding is at least partially dependent on the connections between neighboring functional units such as visual field maps (Allman and Kaas 1974). Van Essen proposed that gyri may form as a result of minimizing the distance between strongly interconnected regions of spatially adjacent functional areas on the brain (Van Essen 1997; Rajimehr and Tootell 2009). For example, the boundary between V1 and V2v is generally on the crown of the lingual gyrus. As the boundary between these regions occurs where the polar angle preference reverses, locations on opposite sides of this gyrus represent the same point in the visual field. Such an arrangement minimizes the connection length between portions of adjacent maps (V1 and V2v) coding for the same location in retinal space.

In the case of intermediate visual areas, it may be that the stronger connectivity between areas sharing an eccentricity representation (such as hV4 and V3) than between areas that belong to separate eccentricity representations (such as hV4 and VO1) pulls hV4 and VO1 away from one another, contributing to the formation of the ptCoS. We note that this hypothesis suggests an influence on folding at a larger spatial scale than a gyrus (as proposed by Van Essen 1997), as the ptCoS is not only the boundary between hV4 and VO1, but also divides the occipital and temporal lobes. Given that the eccentricity representations associated with the confluent fovea and VO fovea lie on separate lobes, these findings provide support for the proposal that retinotopic maps form

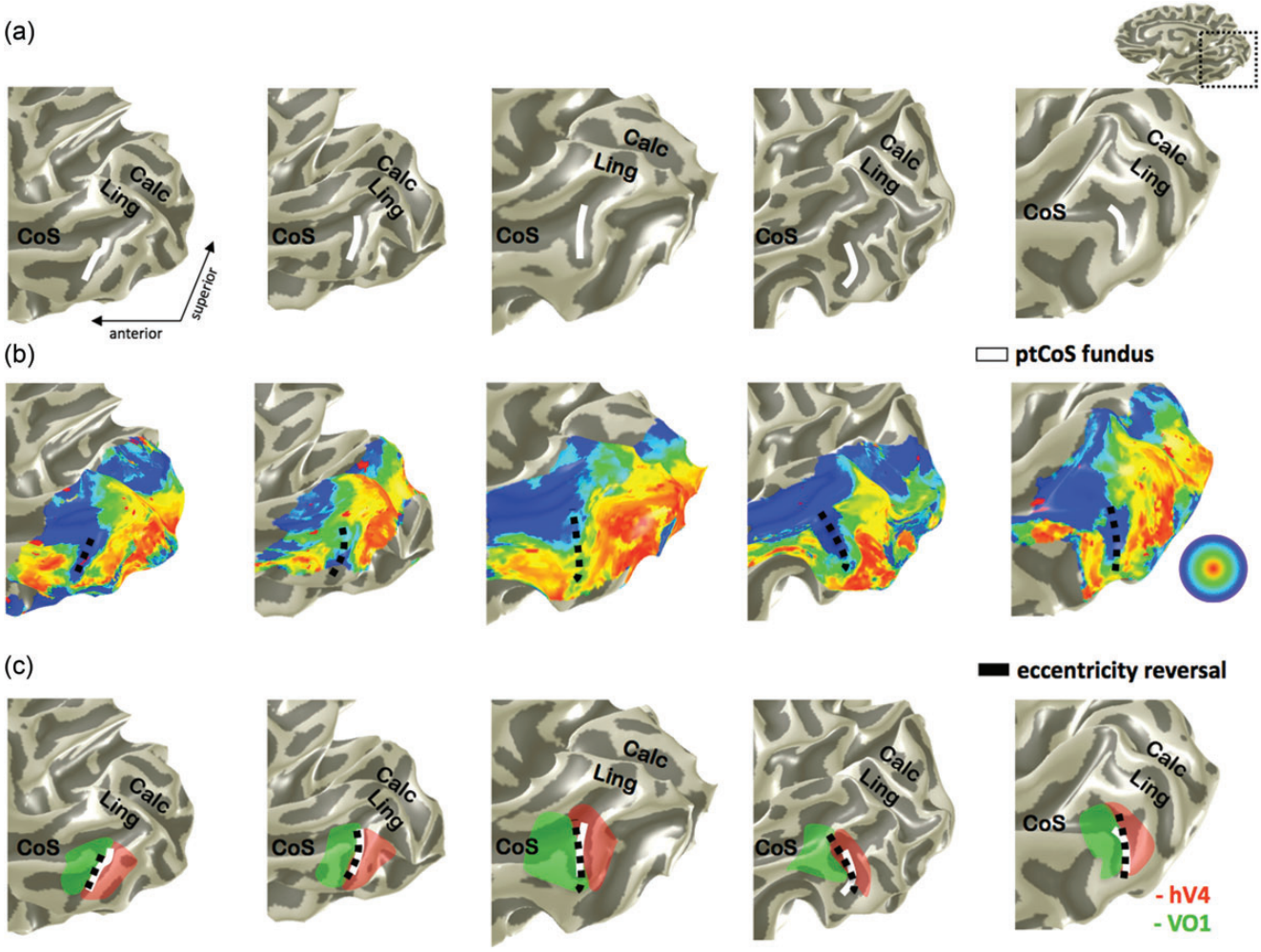

Figure 4. The location of the hV4/VO1 boundary can be reliably predicted from the anatomy alone. (*a*) Ventromedial views of the right hemisphere in 5 subjects from test set 2. The white line represents NW's marking of the location of the fundus of the ptCoS before viewing the retinotopic data. (*b*) The same subjects as shown in (a). In each case, 2 foveas are visible. The black line is eccentricity reversal as marked by KGS before seeing the ptCoS markings in (*a*). (*c*) The same subjects and view as in (*a*) and (*b*), with hV4 (red) and VO1 (green) which were defined using the model in Figure 1. NW's marking of the ptCoS and KGS's marking of the eccentricity reversal are shown superimposed on these visual areas.

computational clusters, with each cluster organized around a distinct fovea (Wandell et al. 2005) and further suggest that each cluster is tied to an anatomical structure. Of course, in the absence of stronger causal evidence, this is a hypothesis, as it is also possible that the existence of the sulcus enforces the boundaries between the maps by affecting the underlying connectivity.

The Arrangement of Retinotopic Preferences with Respect to Cortical Folding may Reflect a Shift in Computation Between V1 and V3 and hV4 and VO1

As noted visual field maps hV4 and VO1 (as well as the maps beyond VO1: VO2 (Brewer et al. 2005), PHC1, and PHC2 (Arcaro et al. 2009) have a different relation to the cortical folding than the V1–V3 visual field maps. In these ventral temporal visual field maps, iso-eccentricity bands are organized roughly parallel to a sulcus (ptCoS for hV4 and VO1, and collateral sulcus for the more anterior maps). Van Essen (1997) hypothesized that spatial proximity between V1 and V2v results from the need for rapid intermap communication among neurons representing the same visual field location across maps. Consequently, the arrangement of hV4, VO1, and the more anterior ventral visual field maps may result from strong within map communication, possibly reflecting the need for spatial integration across large parts of the visual field within a map. Put another way, the arrangements of the maps on the cortical surface may reflect a shift from strongly spatially local computations shared across the posterior visual field maps, to more spatially global computations within the more anterior visual field maps.

In sum, these data show for the first time a robust functional–anatomical correspondence in intermediate areas in the visual hierarchy, with important implications for understanding the relation between cortical folding and functional maps and for defining visual areas from anatomical landmarks alone.

Supplementary Material

Supplementary material can be found at: http://www.cercor.oxfordjournals.org/.

Funding

This research was funded by NEI grants 1RO1 EY0223 1801A1, R01 EY019279-01A1, and NSF grant BCS 0920865 (to K.G.S.) and R01 EY03164 (to Brian Wandell).

Notes

We would like to thank Jonathan Winawer, Hiroshi Horiguchi, Rory Sayres, Kaoru Amano, and Brian Wandell for providing the second data set and Serge Dumoulin for developing the pRF modeling and code. Additionally, Jonathan Winawer helped identify the transverse sinus and along with two anonymous reviewers provided helpful comments on previous drafts. *Conflict of Interest*: None declared.

References

Allman JM, Kaas JH. 1974. The organization of the second visual area (V II) in the owl monkey: a second order transformation of the visual hemifield. Brain Res. 17:247–265.

Arcaro MJ, McMains SA, Singer BD, Kastner S. 2009. Retinotopic organization of human ventral visual cortex. J Neurosci. 29:10638–10652.

Benson NC, Butt OH, Datta R, Radoeva PD, Brainard DH, Aguirre GK. 2012. The retinotopic organization of striate cortex is well predicted by surface topology. Curr Biol. 22:2081–2085.

Bouvier SE, Engel SA. 2006. Behavioral deficits and cortical damage loci in cerebral acrhomatopsia. Cereb Cortex. 16:183–191.

Brewer AA, Liu J, Wade AR, Wandell BA. 2005. Visual field maps and stimulus selectivity in human ventral occipital cortex. Nat Neurosci. 8:1102–1109.

Dougherty RF, Koch VM, Brewer AA, Fischer B, Modersitzki J, Wandell BA. 2003. Visual field representations and locations of visual areas V1/2/3 in human visual cortex. J Vis. 3:586–598.

Dumoulin SO, Bittar RG, Kabani NJ, Baker CL, Le Goualher G, Bruce Pike G, Evans AC. 2000. A new anatomical landmark for reliable identification of human area V5/MT: a quantitative analysis of sulcal patterning. Cereb Cortex. 10:454–463.

Dumoulin SO, Wandell BA. 2008. Population receptive field estimates in human visual cortex. Neuroimage. 39:647–660.

Duvernoy HM, Cabanis EA, Vannson JL. 1991. The human brain: surface, three-dimensional sectional anatomy and MRI. Wein, New York: Springer-Verlag.

Engel SA, Rumelhart DE, Wandell BA, Lee AT, Glover GH, Chichilnisky EJ, Shadlen MN. 1994. fMRI of human visual cortex. Nature. 369:525.

Glover GH, Law CS. 2001. Spiral-in/out BOLD fMRI for increased SNR and reduced suspectbility artifacts. Magn Reson Med. 46:515–522.

Hadjikhani N, Liu AK, Dale AM, Cavanagh P, Tootell RBH. 1998. Retinotopy and color sensitivity in human visual cortical area V8. Nature. 1:235–41.

Hansen KA, Kay KN, Gallant JL. 2007. Topographic organization in and near human visual area V4. J Neurosci. 27:11896–11911.

Hasnain MK, Fox PT, Woldorff MG. 2001. Structure-function spatial covariance in the human visual cortex. Cereb Cortex. 11:702–716.

Huntgeburth SC, Petrides M. 2012. Morphological patterns of the collateral sulcus in the human brain. Eur J Neurosci. 35: 1295–1311.

Kanwisher N, McDermott J, Chun MM. 1997. The fusiform face area: a module in human extrastriate cortex specialized for face perception. J Neurosci. 17:4302–4311.

Levy I, Hasson U, Avidan G, Hendler T, Malach R. 2001. Center-periphery organization of human object areas. Nat Neurosci. 4:533–539.

McKeefry DJ, Zeki S. 1997. The position and topography of the human colour centre as revealed by functional magnetic resonance imaging. Brain. 120:2229–2242.

Meadows JC. 1974. Disturbed perception of colours associated with localized cerebral lesions. Brain. 97:615–632.

Rademacher J, Caviness VS, Steinmetz H, Galaburda AM. 1993. Topographical variation of the human primary cortices: implications for neuroimaging, brain mapping, and neurobiology. Cereb Cortex. 3:313–329.

Rajimehr R, Tootell RBH. 2009. Does retinotopy influence cortical folding in primate visual cortex? J Neurosci. 29:11149–11152.

Sayres R, Grill-Spector K. 2008. Relating retinotopic and object-selective responses in human lateral occipital cortex. J. Neurophysiol. 100:249–267.

Sereno MI, Dale AM, Reppas JB, Kwong KK, Belliveau JW, Brady TJ, Rosen BR, Tootell RBH. 1995. Borders of multiple visual areas in humans revealed by functional magnetic resonance imaging. Science. 268:889–893.

Tyler CW, Likova LT, Chien-Chung C, Kontsevich LL, Schira MM, Wade AR. 2005. Extended concepts of occipital retinotopy. Curr Med Imag Rev. 1:319–329.

Van Essen DC. 1997. A tension-based theory of morphogenesis and compact wiring in the central nervous system. Nature. 385: 313–318.

Wandell BA, Brewer AA, Dougherty RF. 2005. Visual field map clusters in human cortex. Philos TransR Soc Lond. 360:693–707.

Weiner KS, Grill-Spector K. 2010. Sparsely-distributed organization of face and limb activations in human ventral temporal cortex. Neuroimage. 52:1559–1573.

Winawer J, Horiguchi H, Sayres RA, Amano K, Wandell BA. 2010. Mapping hV4 and ventral occipital cortex: the venous eclipse. J Vis. 10:1–22.